HEAT TRANSFER IN A CHANNEL WITH INCLINED TARGET SURFACE COOLED BY SINGLE ARRAY OF CENTERED IMPINGING JETS

by

Ali A. AL MUBARAK*, Syed M. SHAAHID, and Luai M. AL-HADHRAMI

Center for Engineering Research, Research Institute, King Fahd University of Petroleum and Minerals, Dhahran, Saudi Arabia

Original scientific paper
DOI: 10.2298/TSCI110630010A

An experimental investigation has been carried out to study the heat transfer characteristics in a channel with heated target plate inclined at an angle cooled by single array of equally spaced centered impinging jets for jet Reynolds numbers, Re = = 9300, 14400, and 18800. Air ejected from an array of orifices impinges on the heated target surface. The target plate forms the leading edge of a gas turbine blade cooled by jet impingement technique. The work includes the effect of jet Reynolds numbers and feed channel aspect ratios (H/d = 5, 7, and 9 where H = 2.5, 3.5, and 4.5 cm, and d = 0.5 cm) on the heat transfer characteristics for a given orifice jet plate configuration with equally spaced centered holes with outflow exiting in both directions (with inclined heated target surface). In general, It has been observed that, H/d = 9 gives the maximum heat transfer over the entire length of the target surface as compared to all feed channel aspect ratios. H/d = 9 gives 3% more heat transfer from the target surface as compared to H/d = 5 (for Re = 14400). Also, it has been observed that the magnitude of the averaged local Nusselt number increases with an increase in the jet Reynolds number for all the feed channel aspect ratios studied.

Key words: *jet impingement, Reynolds number, Nusselt number, gas turbine*

Introduction

Impingement heat transfer with high velocity gas jets has become an established method of convectively cooling surfaces in a wide variety of process and thermal applications. Examples include cooling of gas turbine airfoils and electronic equipment. In modern gas turbine design, the trend is toward high inlet gas temperature (1600-1800 K) for improving thermal efficiency and power density. Since these temperatures are far above the allowable metal temperature, the gas turbine blades must be cooled in order to operate without failure. Broad range of parameters affect the heat transfer distribution, like impinging jet Re, jet size, target surface geometry, spacing of the target surface from the jet orifices, orifice-jet plate configuration, outflow orientation, *etc*. Literature indicates that some of these parameters have been studied in appreciable depth [1-27].

Chupp *et al*. [1] studied the heat transfer characteristics for the jet impingement cooling of the leading edge region of a gas turbine blade. Flourscheutz *et al*. [2] investigated the heat transfer characteristics of jet array impingement with the effect of initial cross-flow. Metzger and Bunker [3] and Flourscheutz *et al*. [4] used the liquid crystal technique to study the

* Corresponding author; e-mail: mubakali@kfupm.edu.sa

local heat transfer coefficients. The authors observed that the jet Nusselt number depends mainly on the jet Reynolds number.

Dong *et al.* [5] determined experimentally the heat transfer characteristics of a premixed butane/air flame jet impinging upwards on an inclined flat plate at different angles of inclination and fixed Reynolds number (Re = 2500) and a plate to nozzle distance of 5*d*. It was found that the location of maximum heat flux shifted away from impingement point by reducing the angle of incidence. Decreasing the angle of incidence reduced the average heat transfer. Rasipuram and Nasr [6] studied air jet issuing out of defroster's nozzles and impinging on inclined windshield of a vehicle. The overall heat transfer coefficient of the inclined surface for the configuration with one rectangular opening was found to be 16% more than that for the configuration with two rectangular openings. Beitelmal *et al*. [7] investigated the effect of inclination of an impinging air jet on heat transfer characteristics. They found that maximum heat transfer shifts towards the uphill side of the plate and the maximum Nusselt number decreases as the inclination angle decreases. Roy and Patel [8] studied the effect of jet angle impingement on local Nusselt number and nozzle to target plane spacing at different Reynolds number. They found that heat transfer is the maximum through the shear layer formed near the jet attachment stagnation region. Ekkad *et al.* [9] studied the effect of impinging jet angle ±45° on target surface by using transient liquid crystal technique for single Re = $1.28 \cdot 10^4$. It has been noted that the orthogonal jets provide higher Nusselt number as compared to angled jets.

Tawfek [10] investigated the effect of jet inclination on the local heat transfer under an obliquely impinging round air jet striking on circular cylinder. Their results indicated that with increase in inclination, the upstream side of heat transfer profile dropped more rapidly than the downstream side. Seyedein *et al.* [11] performed numerical simulation of two dimensional flow fields and presented the heat transfer due to laminar heated multiple slot jets discharging normally into a converting confined channel by using finite difference method with different Reynolds number (600-1000) and angle of inclination (0-20°). It has been observed that the inclination has a leveling effect on the Nusselt number, distribution over the impingement surface. Yang and Shyu [12] presented numerical predictions of heat transfer characteristics of multiple impinging slot jets with an inclined confinement surface for different angles of inclination and different Reynolds number. The results showed that the local Nusselt number downstream increases with increasing inclination of angle. Yan and Saniei [13] dealt with measurement of heat transfer coefficient of an impinging circular air jet to a flat plate for different oblique angles (45-90°) and different Reynolds number (10000 and 23000) by using transient liquid crystal technique. The results showed that the point of maximum heat transfer shifts away from the geometrical impingement point toward the compression side of the wall jet on the axis of symmetry.

Hwang *et al.* [14] studied the heat transfer in leading edge triangular duct by an array of wall jets with different Reynolds number (3000-12600) and jet spacing *s/d* (1.5-6) by using transient liquid crystal technique on both principal walls forming the apex. Results show that an increase in Reynolds number increases the Nusselt number on both walls. Ramiraz *et al*. [15] investigated the convective heat transfer of an inclined rectangular plate with blunt edge at various Reynolds number (5600-38500) and angle of inclination (60-70°). The heat transfer distribution over a finite rectangular plate was found to be very much dependent on the orientation of the plate. Stevens and Webb [16] examined the effect of jet inclination on local heat transfer under an obliquely impinging round free liquid jet striking at different Reynolds number, angle of inclination, and nozzle sizes. It was found that the point of maximum heat transfer along the x-axis gets shifted upstream.

Hwang and Cheng [17] performed an experimental study to measure local heat transfer coefficients in leading edge using transient liquid crystal technique. Three right triangular ducts of the same altitude and different apex angles (30º, 45º & 60º) were tested for various jet Reynolds number ($3000 \leq Re \leq 12000$) and different jet spacing ($s/d = 3$ and 6). Results show that an increase in Re increases the Nusselt number on all the walls. Hwang and Cheng [18] measured experimentally local heat transfer coefficients on two principal walls of triangular duct with swirl motioned airflow induced by multiple tangential jets from the side entry of the duct by using transient liquid crystal technique. The study indicated that the jet inlet angle affects strongly the averaged bottom-wall heat transfer. Hwang and Chang [19] measured heat transfer coefficients on two walls by using transient liquid crystal technique in triangular duct cooled by multiple tangential jets. The results show that an increase in Reynolds number, increases heat transfer of both walls. Hwang and Cheng [20] studied heat transfer characteristics in a triangular duct cooled by an array of side-entry tangential jets. Detailed heat transfer characteristics were determined (using transient liquid crystal technique) for the two walls forming the apex for different jet Reynolds number and jet spacings. Results showed that an increase in Reynolds number increased the heat transfer on both walls, also a decrease in heat transfer was observed downstream due to cross-flow effect.

It is evident from the earlier published literature that no study has been conducted to show the effect of different jet Reynolds numbers and feed channel aspect ratios (for a given orifice jet plate configuration with equally spaced centered holes with outflow exiting in both directions) on heat transfer in a channel with inclined heated target surface. Therefore, the aim of the present study includes investigation of these effects by conducting the experimental work. Specifically, the work includes the effect of three different jet Reynolds numbers (9300, 14400, and 18800) and feed channel aspect ratios ($H/d = 5$, 7, and 9 where $H = 2.5$, 3.5, 4.5 cm and diameter of jet $d = 0.5$ cm) on the heat transfer characteristics for a given orifice jet plate configuration with equally spaced centered holes with outflow exiting in both directions (with inclined heated target surface). The motivation behind this work is that the channel of turbine blade internal cooling circuit at the leading edge is inclined.

Description of the experiment

The schematic of the experimental set-up is depicted in fig. 1. The test rig used to study the heat transfer characteristics has been constructed using plexiglass. The test section consists of two channels, impingement (10) and the feed channel (9). Air enters the test section in the feed channel and is directed onto the heated copper plates in the impingement channel to study the heat transfer characteristics. The target plates (11), made of copper, were heated using a constant flux heater. The other side of the heater was insulated to get the heat transferred only in one direction. The mass flow rate of the compressed air (1) entering the test section was passed through a settling chamber (5) and was controlled with the help of valves (2). The pressure drop was measured using the pressure gauges (4). Gas flow meter (7) was used to measure the mass flow rate entering the test rig which was protected by the air filters (6) of 50 capacity.

The average surface temperature of each copper plate was determined from the readings of two T-type thermocouples (12) installed in the holes drilled at the back surface of the plates to within 1 mm of the surface in depth. The analog signals generated by these temperature sensors were transmitted to the signal-conditioning unit where they were processed. The resulting analog signals were converted into digital signals by a DAQ (13) card and recorded with an application software developed in LabView.

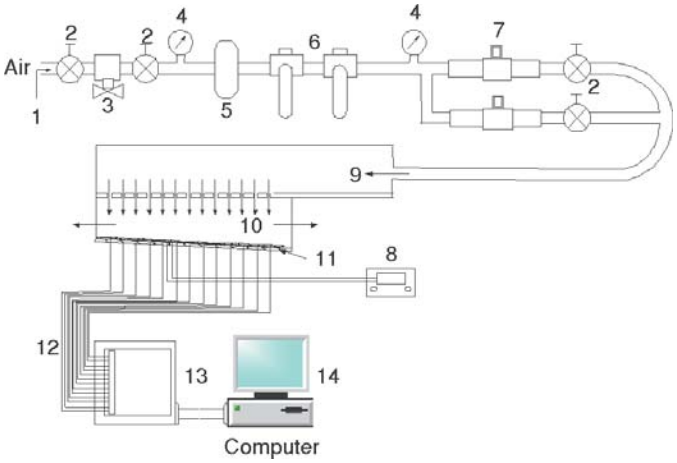

Figure 1. Schematic of the test section
1 – compressed air, 2 – valves, 3 – discharged valve, 4 – pressure gauges, 5 – settling chamber, 6 – air and oil filters, 7 – digital flow meters, 8 – transformer, 9 – feeding channel, 10 – impingement channel, 11 – target surface, 12 – thermocouples, 13 – data acquisition , 14 – computer

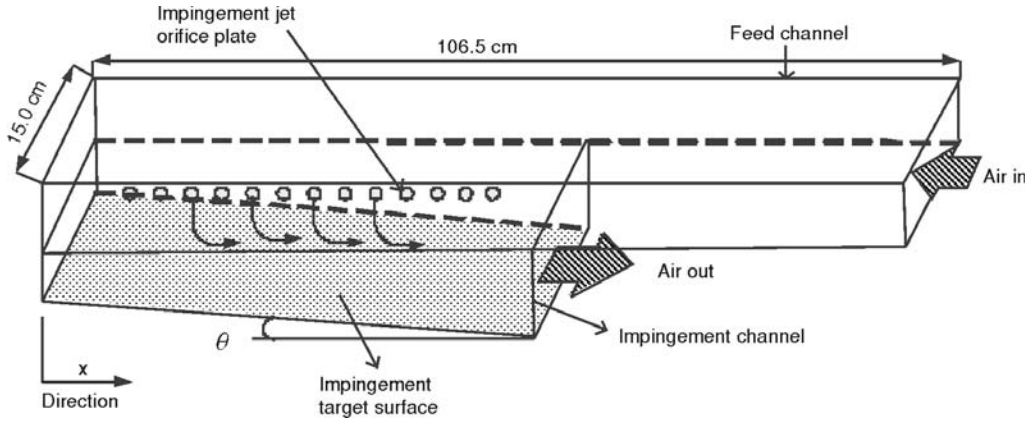

Figure 2.1. 3-D view of the test section

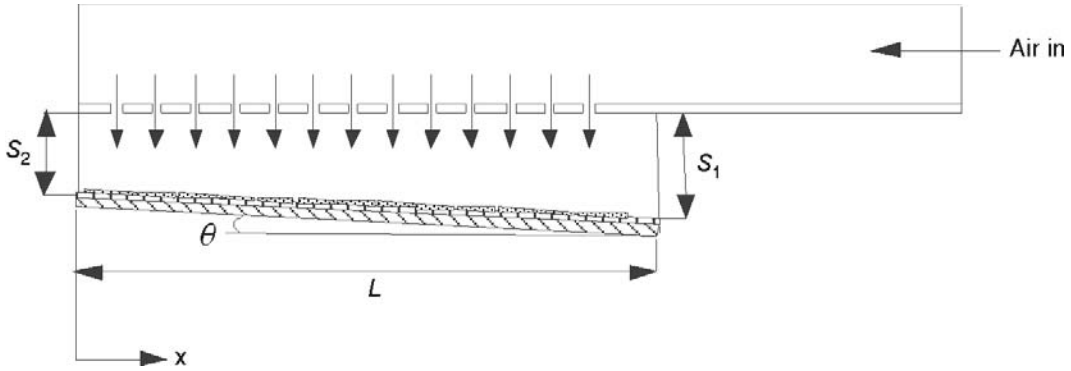

Figure 2.2. Inclination angle of the target surface

Figure 2.1 shows the 3-D sketch of the test section. It consists of two channels joined by the orifice plate, which has a single array of equally spaced centered jets shown in fig. 3. The jet orifice plate thickness is twice the jet diameter. There are 13 jets on the orifice plate. The jet-to-jet spacing is 8 times the jet diameter and the orifice jet diameter $d = 0.5$ cm. The length of the test section is 106.5 cm (fig. 2.1). The width of the feed channel (H) was varied from 2.5 to 4.5 cm (*i. e.* $H/d = 5$, 7, and 9, $d = 0.5$ cm). The impingement target surface constitutes a series of 13 copper plates, each with 4.2×4.1 cm in size, arranged in accordance with the orifice jets such that the impingement jet hits the geometric center of the corresponding plate (however, first and last copper plates are slightly different in sizes). All the copper plates are separated from each other by 1 mm distance to avoid the lateral heat conduction, thus dividing the target surface into segments. The thickness of the copper plate is 0.5 cm. As shown in fig. 2.2, the length of impingement surface L is 57.3 cm (the target surface is inclined at angle 1.5º, the width of parallel flow side "S2" is 2 cm and the width of the opposite flow side "S1" is 3.5 cm).

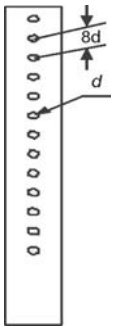

Figure 3. Illustration of orifice-jet configuration with single array equally spaced centered jets (d = 5 mm)

Figure 4 shows the schematic of the three different outflow orientations. The upper channel is called as the feed channel and the lower channel in which the jets impinge on the target surface is called as the impingement channel. The exit of jets in three different outflow orientations from the impingement channel creates different cross-flow effects as shown in fig. 4:

– Case-1 (Outflow coincident with the entry flow),
– Case-2 (Outflow opposing to the entry flow), and
– Case-3 (Outflow passes out in both the directions).

However, in the present study, attention is focused on Case-3.

Figure 5 shows the details of the construction of the target surface. The copper plate is heated with a constant flux heater held between the wooden block and the copper plate by glue (to reduce contact resistance). The ends were sealed with a rubber material to avoid lateral heat losses. The wooden block was 3 cm thick to minimize the heat lost to the surroundings, so that the heat is transferred completely to copper plates only.

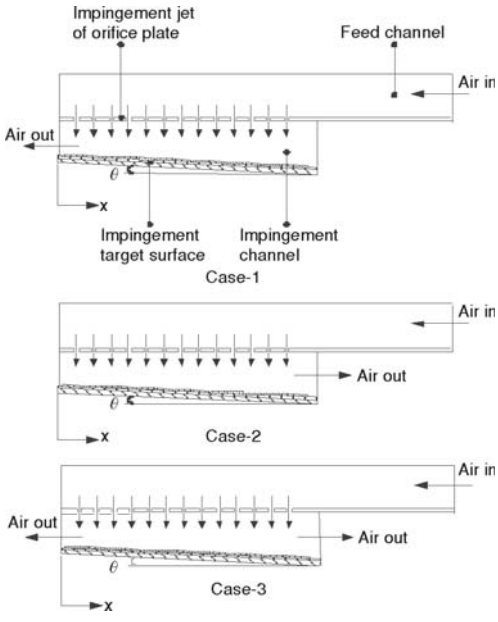

Figure 4. Illustration of three exit outflow orientations

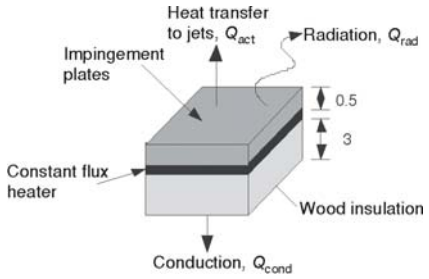

Figure 5. Overall energy balance over a small element of the impingement plate

Procedure

Tests were carried out using a given orifice-jet plate (equally spaced centered holes) with jet diameter $d = 0.5$ cm for a given jet Reynolds number Re = 9300 (for a given H/d ratio, for outflow passing in both directions) and for a constant heat flux power input. The heated target plate was oriented at a pre-defined angle (1.5º). The mass flow rate was adjusted to the required value for the experiment to be conducted and the air was blown continuously into the test section. Heat was supplied to the copper plates with electric resistive constant flux heaters from backside to provide uniform heat flux. The temperature of the copper plates was measured by two thermocouples mounted in a groove of 2.5 mm on the back of the copper plates. Thus the temperature of a particular plate has been taken as the average of the reading of two thermocouples. The temperature of the copper plates, pressure, temperature of the air at the inlet, and the mass flow rate were continuously monitored. After the temperature of the copper plates reached the steady-state condition, all the data was collected with LabVIEW program. The Nusselt number was then calculated based upon the collected data. The same procedure was repeated for three different jet Reynolds numbers (Re = 9300, 14400, and 18800) and for different aspect ratios (H/d = 5, 7, and 9) for a given orifice jet plate configuration with equally spaced centered holes with outflow exiting in both directions (with inclined heated target surface).

Data reduction and uncertainty analysis

The collected data was subjected to uncertainty analysis. The method for performing the uncertainty analysis for the present experimental investigation has been taken from Taylor [21]. The theory for the current uncertainty analysis is summarized in the following discussion.

Jet Reynolds number calculations

The average velocity used to calculate the jet Reynolds number is calculated using the equation:

$$V_{\text{avg}} = \frac{\forall}{13\frac{\pi}{4}d^2} \tag{1}$$

The data reduction equation for the jet Reynolds number is taken as:

$$\text{Re} = \frac{\rho V_{\text{avg}} d}{\mu} = \frac{\rho d}{\mu}\frac{\forall}{13\frac{\pi}{4}d^2} \tag{2}$$

Uncertainty in jet Reynolds number

Taking into consideration only the measured values, which have significant uncertainty, the jet Reynolds number is a function of orifice jet diameter and volume flow rate and is expressed mathematically as:

$$\text{Re} = f(\forall, d) \tag{3}$$

Density and dynamic viscosity of air is not included in the measured variables since it has negligible error in the computation of the uncertainty in jet Reynolds number. The uncertainty in Reynolds number has been found to be about 2.2 %.

Nusselt number calculation

The total power input to all the copper plates was computed using the voltage and current, the former being measured across the heater, using the equation:

$$Q_{\text{total}} = \frac{V^2}{R} = VI \tag{4}$$

The heat flux supplied to each copper plate was calculated using:

$$q'' = \frac{Q_{\text{total}}}{A_{\text{total}}} \tag{5}$$

The heater gives the constant heat flux for each copper plate. The heat supplied to each copper plate from the heater is calculated using the procedure:

$$Q_{\text{cp,i}} = q'' A_{\text{cp,i}} \tag{6}$$

where i is the index number for each copper plate. The heat lost by conduction through the wood and to the surrounding by radiation is depicted in fig. 5 and has been estimated using the equations for each plate:

$$Q_{\text{cond,i}} = k_{\text{wood}} A_{\text{cp,i}} \frac{T_{\text{s,i}} - T_{\text{w}}}{t} \tag{7}$$

$$Q_{\text{rad,i}} = \varepsilon\sigma A_{\text{cp,i}} (T_{\text{s,i}}^4 - T_{\text{surr}}^4) \tag{8}$$

The actual heat supplied to each copper plate has been determined by deducting the losses from the total heat supplied to the heater:

$$Q_{\text{actual, i}} = Q_{\text{cp, i}} - (Q_{\text{cond, i}} + Q_{\text{rad, i}}) \tag{9}$$

The local convective heat transfer coefficient for each of the copper plate has been calculated using:

$$h_{\text{i}} = \frac{Q_{\text{actual,i}}}{A_{\text{cp,i}} (T_{\text{s,i}} - T_{\text{in}})} \tag{10}$$

The average temperature of the heated target surface $T_{\text{s,i}}$ has been taken as the average of the readings of two thermocouples fixed in each copper plate. To calculate h, T_{in} has been considered instead of the bulk temperature or the reference temperature. For a given case (for a given Re, H/d, and orifice-jet plate) T_{in} is fixed. It is measured at the test section inlet, where the air first enters the feed channel. The non-dimensional heat transfer coefficient on the impingement target surface is represented by Nusselt number as:

$$\text{Nu}_i = \frac{h_i d}{k_{\text{air}}} \tag{11}$$

The hydraulic diameter has been taken as the diameter of the orifice jet. The data reduction equation for the Nusselt number is considered along with the heat losses by conduction and radiation:

$$\text{Nu}_i = \frac{d}{k_{\text{air}}} \left(\frac{\dfrac{V^2}{RA_{\text{total}}} - \dfrac{k_{\text{w}}}{w}(T_{\text{s,i}} - T_{\text{w}}) - \varepsilon\sigma(T_{\text{s,i}}^4 - T_{\text{surr}}^4)}{T_{\text{s,i}} - T_{\text{in}}} \right) \tag{12}$$

Uncertainty in Nusselt number

Temperature of the wood has a very little effect on the uncertainty of heat transfer coefficient due to the large thickness of the wood and also due to the insulation material attached to

the wooden block. Temperature of the surroundings and emissivity also has less effect on the uncertainty as the work was carried out in a controlled environment and the temperature of the surroundings was maintained within 21-23 °C through out the experiment. The standard uncertainty in the Nusselt number neglecting the covariance has been calculated using the equation:

$$(U_{c,Nu_i})^2 = \left(\frac{\partial \mathrm{Nu}_i}{\partial V} u_\mathrm{V}\right)^2 + \left(\frac{\partial \mathrm{Nu}_i}{\partial R} u_\mathrm{R}\right)^2 + \left(\frac{\partial \mathrm{Nu}_i}{\partial T_{s,i}} u_{\mathrm{T_{s,i}}}\right)^2 + \left(\frac{\partial \mathrm{Nu}_i}{\partial T_{in}} u_{\mathrm{T_{in}}}\right)^2 + \left(\frac{\partial \mathrm{Nu}_i}{\partial A_\mathrm{total}} u_{\mathrm{A_{total}}}\right)^2 + \left(\frac{\partial \mathrm{Nu}_i}{\partial d} u_\mathrm{d}\right)^2 \quad (13)$$

Uncertainty propagation for the dependent variable in terms of the measured values has been calculated using the Engineering Equation Solver (EES) software. The measured variables $x_1, x_2, etc.$ have a random variability that is referred to as its uncertainty. The uncertainty in Nusselt number in the present study has been found to vary between ± 6% depending upon the jet velocity.

Results and discussions

Jet impingement heat transfer is dependent on several flow and geometrical parameters. The jet impingement Nusselt number is presented in a functional form as follows:

$$\mathrm{Nu}_i = \frac{h_i d}{k_\mathrm{air}} = f\left[\begin{matrix}\mathrm{Re}, \left(\frac{X}{d}, \frac{H}{d}\right) \\ \text{out flow orientation}\end{matrix}\right] \quad (14)$$

where, Reynolds number is the flow parameter, jet spacing to the diameter ratio (X/d) is the geometric parameter. The flow exit direction and target surface geometry are also important parameters having a considerable impact on impingement heat transfer.

The X location starts from the supply end of the channel as shown in fig. 2.1. For the case 1 shown in fig. 4(a), flow enters at X/d = 109.3 and exits at X/d = 0. For case 2. fig. 4(b), flow exits at X/d = 109.3. For case 3. fig. 4(c), flow exits at both ends (X/d = 0 and X/d = 109.3). The flow is fully developed before entering the orifice jets. However, in the present study attention is focused on Case-3 (out-flow passing out in both directions).

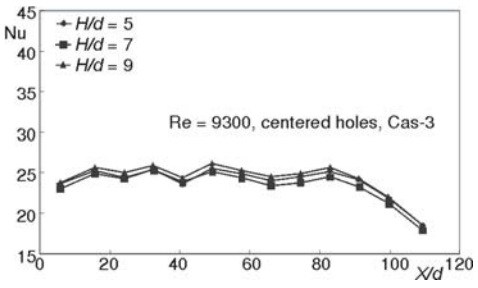

Figure 6. Nusselt number variation for different aspect ratios and for outflow passing in both directions (for jet-orifice plate with centered holes and for Re = 9300)

Effect of jet Reynolds number and feed channel aspect ratio on local Nusselt number

Figures 6-8 show the local Nusselt number distribution for three Reynolds numbers (Re = 9300, 14400, and 18800) and for three H/d ratios (H/d = 5, 7, and 9 where H = 2.5, 3.5, and 4.5 cm and d = 0.5 cm) as a function of non-dimensional location X/d on the heated target surface (for outflow passing in both directions as shown in fig. 4(c), and for a given orifice-jet plate with centered holes. In general, it has been observed that the H/d profiles overlap each other at some points on the target plate (this is due to inter mixing of jets).

Figure 6 shows the effect of feed channel aspect ratio (*H/d*) on local Nusselt number for Re = 9300 for orifice jet plate with centered holes with outflow passing in both directions. It can be observed that, *H/d* = 9 gives the maximum heat transfer over the entire length of the target surface as compared to all feed channel aspect ratio studied. *H/d* = 9 gives 2% more heat transfer from the target surface as compared to *H/d* = 5. Whereas *H/d* = 5 gives a maximum of 2% increase in heat transfer as compared to *H/d* = 7. The cross-flow boundary layer and jet strength almost equal over the entire target surface so the heat transfer is almost the same.

Figure 7 shows the effect of feed channel aspect ratio (*H/d*) on local Nusselt number for Re = 14400 for orifice jet plate with centered jets with outflow passing in both directions. It can be observed that, *H/d* = 9 gives the maximum heat transfer over the entire length of the target surface as compared to all feed channel aspect ratio studied. *H/d* = 9 gives 2% more heat transfer from the target surface compared to *H/d* = 7. Whereas *H/d* = 7 gives a maximum of 1% increase in heat transfer as compared to *H/d* = 5.

Figure 8 shows the effect of feed channel aspect ratio (*H/d*) on local Nusselt number for Re = 18800 for orifice jet plate with centered jets with outflow passing in both directions. It can be observed that, *H/d* = 9 gives the maximum heat transfer over the entire length of the target surface as compared to other feed channel aspect ratio studied. *H/d* = 9 gives 1% more heat transfer from the target surface compared to *H/d* = 5. Whereas *H/d* = 5 gives a maximum of 1% increase in heat transfer as compared to *H/d* = 7.

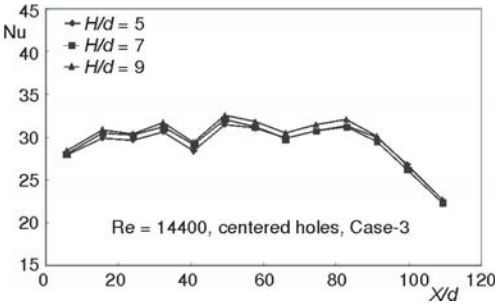

Figure 7. Nusselt number variation for different aspect ratios and for outflow passing out in both directions (for jet-orifice plate with centered holes and for Re = 14400)

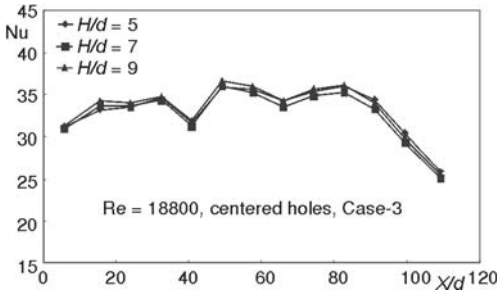

Figure 8. Nusselt number variation for different aspect ratios and for outflow passing in both directions (for jet-orifice plate with centered holes and for Re = 18800)

Effect of jet Reynolds number and feed channel aspect ratio on averaged Nusselt number

The average Nusselt number is the average of Nusselt number of all 13 copper plates on the target surface for a given situation (*i. e.* for a given Reynolds number, *H/d*, orifice-jet configuration, outflow orientation).

Figure 9 shows the effect of different feed channel aspect ratios (*H/d*) on average Nusselt number for different jet Reynolds numbers for outflow passing out in both directions, Case-3, fig. 4(c), and for orifice-jet plate with centered holes. The Nusselt number has been found to increase with increase in Reynolds number. In general, the percentage increase in average Nusselt number in going from *H/d* = 5 to *H/d* = 7 or from *H/d* = 7 to *H/d* = 9 is not much. However, *H/d* = 9 gives slightly higher average Nusselt number as compared to *H/d* = 7 and *H/d* = 5. Also, The Nusselt number has been found to increase with increase in Reynolds number for all the aspect ratios.

It is difficult to find out the exact experimental set-up in the literature which has been developed in the present study for comparison of results, however, attempt has been made to make some comparison. Figure 10 compares the results of the present study with archival results of Huang *et al*. [22] for different jet Reynolds number and for different outflow orientations (for a given jet-orifice plate with centered jets). Huang's study focused on multiple array jets, however our study concentrated on single array of centered jet swith outflow passing out in both directions (with an inclined target surface). Florschuetz [4] studied experimentally heat transfer distributions for jet array impingement. He considered circular jets of air impinging on heat transfer surface parallel to the jet orifice plate. The air after impingement was constrained in a single direction. Florschuetz presented Nu for centered and staggered hole patterns.

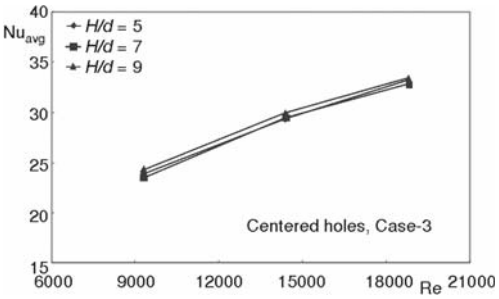

Figure 9. Average Nusselt number distribution for different jet Reynolds number and for different feed channel aspect rations (for jet-orifice plate with centered holes, for outflow passing out in both directions – Case-3)

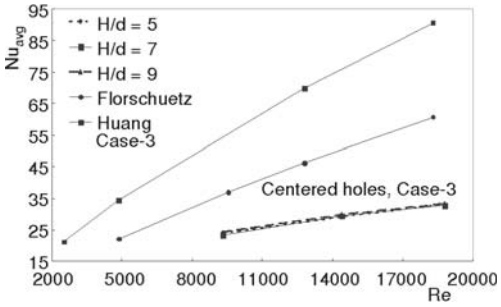

Figure 10. Comparison of average Nusselt number of present study with other studies for different jet Reynolds number and for different feed channel aspect ratios (for orifice jet-plate with centered holes, outflow in both directions)

Conclusions

The study has discussed in appreciable depth the effect of jet Reynolds numbers (Re = = 9300, 14400, and 18800) and feed channel aspect ratios (H/d = 5, 7, and 9 where H = 2.5, 3.5, and 4.5 cm, and d = 0.5 cm) on the heat transfer characteristics for a given orifice jet plate configuration with equally spaced centered holes with outflow exiting in both directions (with inclined heated target surface). In general, it has been observed that Nusselt number is high for higher aspect ratios. For a given plate with single array of equally spaced centered jets and for Re = 14400 (out flow passing in both directions), the local Nusselt number for H/d = 9 has been found to be greater than Nusselt number of H/d = 5 by 3%. Also, it has been observed that the magnitude of the averaged Nusselt number increases with increase in jet Reynolds number for all the aspect ratios. The observations of the present experimental work offer valuable information for researchers and designers.

Acknowledgment

The present work was supported by Research Institute, King Fahd University of Petroleum and Minerals, Dhahran, Saudi Arabia. The authors would like to greatly appreciate the above support. without such support, this work would not have been possible.

Nomenclature

$A_{cp,i}$ – area of each copper plate, [m^2]
A_{total} – area of all copper plate, [m^2]
d – diameter of the orifice jet, [m]
H – width of the feed channel, [m]

h_i – local convective heat transfer co-efficient, [$Wm^{-2}K^{-1}$]
I – current supplied to heater, [A]
l – length of the copper plate, [m]
k_{air} – thermal conductivity of air, [$Wm^{-1}K^{-1}$]
k_{wood} – thermal conductivity of wood, [$Wm^{-1}K^{-1}$]
Nu_i – local Nusselt number for each copper plate
Nu_{avg} – average Nusselt number
$Q_{cp,i}$ – heat input for each copper plate, [W]
Q_{actual} – actual heat released from target surface, [W]
$Q_{cond,i}$ – heat lost due to conduction, [W]
$Q_{rad,i}$ – heat lost due to radiation, [W]
Q_{total} – total heat input, [W]
q'' – heat flux from the heater, [Wm^{-2}]
R – resistance of the heater, [Ω]
Re – jet Reynolds number
T_{in} – inlet temperature, [ºC]
$T_{s,i}$ – surface temperature, [ºC]
T_{surr} – temperature of the surroundings, [ºC]
T_w – wood block temperature, [ºC]
t – thickness of wood block behind the heater, [m]
U – uncertainty
V – voltage supplied to the heater, [V]
V_{avg} – average velocity of all jets, [ms^{-1}]
$\forall$ – volume flow rate, [m^3s^{-1}]
X – distance in the x-direction, [m]

Greek symbols

ε – emissivity
θ – inclination angle [1.5º]
μ – dynamic viscosity [$kgm^{-1}s^{-1}$]
ρ – density, [kgm^{-3}]
σ – Stefan-Boltzman constant, [$Wm^{-2}K^{-4}$]

Subscripts

cp – copper plate
i – index number for each copper plate
j – jet
w – wood

References

[1] Chupp, R. E., *et al*., Evaluation of Internal Heat-Transfer Coefficients for Impingement-Cooled Turbine Airfoils, *J. Aircraft, 6* (1969), 3, pp. 203-208
[2] Florschuetz, L. W., *et al*., Heat Transfer Characteristics for Jet Array Impingement with Initial Cross Flow, *Journal of Heat Transfer, 106* (1984), 1, pp. 34-41
[3] Metzger, D. E., Bunker, R. S., Local Heat Transfer in Internally Cooled Turbine Airfoil Leading Edge Regions: Part I – Impingement Cooling without Film Coolant Extraction, *Journal of Turbo Machinery, 112* (1990), 3, pp. 451-458
[4] Florschuetz, L. W., *et al*., Stream-Wise Flow and Heat Transfer Distributions for Jet Impingement with Cross Flow, *Journal of Heat Transfer, 103* (1981), 2, pp. 337-342
[5] Dong, L. L., *et al*., Heat Transfer Characteristics of Premixed Butane/Air Flame Jet Impinging on an Inclined Flat Surface, *Heat and Mass Transfer, 39* (2002), 1, pp. 19-26
[6] Rasipuram, S. C., Nasr, K. J., A Numerically-Based Parametric Study of Heat Transfer off an Inclined Surface Subject to Impinging Air Flow, *International Journal of Heat and Mass Transfer, 47* (2004), 23, pp. 4967-4977
[7] Beitelmal, A. H., *et al*., Effect of Inclination on the Heat Transfer between a Flat Surface and an Impinging Two-Dimensional Air Jet, *International Journal of Heat and Fluid Flow, 21* (2000), 2, pp. 156-163
[8] Roy, S., Patel, P. Study of Heat Transfer for a Pair of Rectangular Jets Impinging on an Inclined Surface, *International Journal of Heat and Mass Transfer, 46* (2003), 3, pp. 411-425
[9] Ekkad, S., *et al*., Impingement Heat Transfer Measurements under an Array of Inclined Jets, *Journal of Thermophysics and Heat Transfer, 14* (2000), 2, pp. 286-288
[10] Tawfek, A. A., Heat Transfer Studies of the Oblique Impingement of Round Jets Upon a Covered Surface, *Heat and Mass Transfer, 38* (2002), 6, pp. 467-475
[11] Seyedein, S. H., *et al*., Laminar Flow and Heat Transfer from Multiple Impinging Slot Jets with an Inclined Confinement Surface, *International Journal of Heat and Mass Transfer, 37* (1994), 13, pp. 1867-1875
[12] Yang, Y., Shyu, C. H., Numerical Study of Multiple Impinging Slot Jets with an Inclined Confinement Surface, *Numerical Heat Transfer; Part A: Applications, 33* (1998), 1, pp. 23-37
[13] Yan, X., Saniei, N., Heat Transfer from an Obliquely Impinging Circular Air Jet to a Flat Plate, *International Journal of Heat and Fluid Flow, 18* (1997), 6, pp. 591-599
[14] Hwang, J. J., *et al*., Jet-Spacing Effect on Impinged Heat Transfer in a Triangular Duct with a Tangential Jet-Array, *International Journal of Transfer Phenomena, 5* (2003), 1, pp. 65-74
[15] Ramirez, C., *et al*., Convective Heat Transfer of an Inclined Rectangular Plate, *Experimental Heat Transfer, 15* (2002), 1, pp. 1-18

[16] Stevens, J., Webb, B. W., Effect of Inclination on Local Heat Transfer Under an Axisymmetric Free Liquid Jet, *International Journal of Heat and Mass Transfer, 34* (1991), 4-5, pp. 1227-1236
[17] Hwang, J. J., Cheng, C. S., Impingement Cooling in Triangular Ducts Using an Array of Side-Entry Wall Jets, *International Journal of Heat and Mass Transfer, 44* (2001), 5, pp. 1053-1063
[18] Hwang, J.J., Cheng, T. T., Augmented Heat Transfer in a Triangular Duct by Using Multiple Swirling Jets, *Journal of Heat Transfer, 121* (1999), pp. 683-690
[19] Hwang, J. J., Chang, Y., Effect of Outflow Orientation on Heat Transfer and Pressure Drop in a Triangular Duct with an Array of Tangential Jets, *Journal of Heat Transfer, 122* (2000), 4, pp. 669-678
[20] Hwang, J.J., Cheng, C. S., Detailed Heat Transfer Distributions in a Triangular Duct with an Array of Tangential Jets, *Journal of Flow Visualization & Image Processing, 6* (1999), 2, pp. 115-128
[21] Taylor, B. N., Kuyatt, C. E., Guidelines for Evaluating and Expressing the Uncertainty of NIST Measurement Results, National Institute of Standards and Technology, NIST Technical Note 1297, Gaithersburg, Md., USA, 1994
[22] Hwang, Y., *et al.*, Detailed Heat Transfer Distributions Under an Array of Orthogonal Impinging Jets, *Journal of Thermophysics and Heat Transfer, 12* (1998), 1, pp. 73-79
[23] Yan, W. M., *et al*., Experimental Study of Impingement Heat Transfer of Inline and Staggered Jet Arrays by Using Transient Liquid Crystal Technique, *J. Flow Visualization and Image Processing, 10* (2003), 1-2, pp. 119-141
[24] Yan, W. M., *et al.*, Measurement of Detailed Heat Transfer on a Surface under Arrays of Impinging Elliptic Jets by a Transient Liquid Crystal Technique, *Int. J. Heat Mass Transfer, 47* (2004), 24, pp. 5235-5245
[25] Yan, W. M., *et al*., Experimental Study of Impinging Heat Transfer along Rib-Roughened Walls by Using Transient Liquid Crystal Technique, *Int. J. Heat Mass Transfer, 48* (2005), 12, pp. 2420-2428
[26] Yan, W. M., Mei, S. C., Measurement of Detailed Heat Transfer Along Rib-Roughened Surface under Arrays of Impinging Elliptic Jets, *Int. J. Heat Mass Transfer, 49* (2006), pp. 157-170
[27] Jang, J. H., *et al*., Experimental Study on the Heat Transfer under Impinging Elliptic Jet Array along a Film Hole Surface Using Liquid Crystal Thermograph, *Int. J. Heat Mass Transfer, 52* (2009), 19-20, pp. 4435-4448

Paper submitted: June 30, 2011
Paper revised: December 28, 2011
Paper accepted: January 6, 2012